Consistency evaluation of tropospheric ozone from ozonesonde and IAGOS aircraft observations: vertical distribution, ozonesonde types and station-airport distance

Honglei Wang[1, 2], David W. Tarasick[3*], Jane Liu[2*], Herman G.J. Smit[4], Roeland Van Malderen[5], Lijuan Shen[6], Romain Blot[7], Tianliang Zhao[1]

[1] China Meteorological Administration Aerosol-Cloud and Precipitation Key Laboratory, Nanjing University of Information Science and Technology, Nanjing, 210044, China

[2] Department of Geography and Planning, University of Toronto, Toronto, M5S 3G3, Canada

[3] Environment and Climate Change Canada, 4905 Dufferin Street, Downsview, M3H 5T4, Canada

4 Institute for Energy and Climate Research: Troposphere (IEK-8), Research Centre Juelich (FZJ), Juelich, Germany

[5] Royal Meteorological Institute of Belgium, Brussels, Belgium

[6] School of Atmosphere and Remote Sensing, Wuxi University, Wuxi, 214105, China

[7] Laboratoire d'Aérologie (LAERO), Université de Toulouse, CNRS, Toulouse, France

* Corresponding authors: David.Tarasick@ec.gc.ca and janejj.liu@utoronto.ca

Abstract: The vertical distribution of tropospheric O_3 from ozonesondes is compared with that from In-service Aircraft for a Global Observing System (IAGOS) measurements at 23 pairs of sites between about 30°S and 55°N, from 1995 to 2021. Profiles of tropospheric O_3 from IAGOS aircraft are in generally good agreement with ozonesonde observations, for Electrochemical concentration cells (ECC), Brewer-Mast, and Carbon-Iodine sensors, with average biases of 2.58 ppb, -0.28 ppb, and 0.67 ppb, and correlation coefficients (R) of 0.72, 0.82, and 0.66, respectively. Agreement between the aircraft and Indian-sonde observations is poor, with an average bias of 15.32 ppb and R of 0.44. The O_3 concentration observed by ECC sondes is on average higher by 5-10% than that observed by IAGOS aircraft, and the relative bias increases modestly with altitude. For other sonde types, there are some seasonal and altitude variations in the relative bias with respect to IAGOS measurements, but these appear to be caused by local differences. The distance between station and airport within 4° has little effect on the comparison results. For the ECC ozonesonde, the overall bias with respect to IAGOS measurements varies from 5.7 to 9.8 ppb, when the station pairs are grouped by station-airport distances of <1° (latitude and longitude), 1-2°, and 2-4°. Correlations for

these groups are R = 0.8, 0.9 and 0.7. These comparison results provide important information for merging ozonesonde and IAGOS measurement datasets. They can also be used to evaluate the relative biases of the different sonde types in the troposphere, using the aircraft as a transfer standard.

Key words: WOUDC; IAGOS; tropospheric O_3; vertical distribution; ozonesonde; aircraft

1 Introduction

Ozone (O_3) is a trace gas with small concentrations in the atmosphere (Ramanathan et al., 1985). It is an important greenhouse gas in the upper troposphere. In the planetary boundary layer, it is a major air pollutant (Lefohn et al., 2018; Monks et al., 2015). It can endanger human health, damage ecosystems, and affect climate change (Fu and Tai, 2015; Lefohn et al., 2018; Percy et al., 2003). Therefore, it is of importance to study the temporal and spatial variations in tropospheric O_3 including near-surface O_3 and mechanisms affecting the variations (Logan, 1985; Ma et al., 2020; Sharma et al., 2017; Young et al., 2018).

A large number of studies have been carried out on the spatiotemporal distribution, formation mechanisms, and transport characteristics of tropospheric O_3 (Li et al., 2020, 2021; Vingarzan, 2004; Wang et al., 2017, 2023; Xu et al., 2021; Yu et al., 2021). However, due to the limitation of observations, there are many unknowns on tropospheric O_3, especially the vertical distribution of tropospheric O_3. Satellites provide an effective platform for measuring O_3 globally. Satellite O_3 instruments, including TES, GOME, GOME-2, SCIAMACHY, OMI, and TROPOMI, have been in operation for decades (David et al., 2013; Ebojie et al., 2016; Hegarty et al., 2009; Hoogen et al., 1999; Hubert et al., 2021; Miles et al., 2015). Although satellite observations can provide detailed temporally- and horizontally-resolved maps of tropospheric O_3 columns, in general satellite data lack vertical resolution. While tropospheric differential absorption lidar can also provide vertical distribution information for tropospheric O_3 (Keckhut et al., 2004; Yang et al., 2023), there are very few routinely operating stations.

The principal sources of vertically-resolved, trend-quality observations of tropospheric O_3 are therefore balloon-borne ozonesondes, and IAGOS aircraft observations. The World Ozone and Ultraviolet Radiation Data Centre (WOUDC) and the In-service Aircraft for a Global Observing System database (IAGOS) house the data from these two observation programs with the longest

duration and the most global stations, which are the most widely used for tropospheric O_3 studies (Gaudel et al., 2020; Liao et al., 2021; Tarasick et al., 2019; Wang et al., 2022; Zang et al., 2024). These two datasets are used to study the distribution, variability and trends of tropospheric O_3, and its sources and transport, as well as satellite and model validation (Hu et al., 2017; Gaudel et al., 2018; 2020; Wang et al., 2022; Zhang et al., 2008). The first phase of the Tropospheric Ozone Assessment Report (TOAR-I), initiated in 2014, utilized available surface, ozonesonde, aircraft, and satellite observations to assess tropospheric O_3 trends from 1970 to 2014 (Schultz et al., 2017). Hu et al. (2017) found that the largest bias in a chemical transport model, GEOS-Chem, with respect to ozonesondes and IAGOS observations, is in high northern latitudes in winter-spring, where the simulated O_3 is 10-20 ppb lower. Wang et al. (2022) examined observed tropospheric O_3 trends, their attributions, and radiative impacts from 1995 to 2017, using aircraft observations from IAGOS, ozonesondes, and a multi-decadal GEOS-Chem chemical model simulation, and found increases in tropospheric O_3 (950-250 hPa) of 2.7 ± 1.7 ppbv per decade from IAGOS observations in the Northern Hemisphere and at 19 of 27 global ozonesonde sites averaging 1.9 ± 1.7 ppbv per decade. There are also a number of comparative studies on these two datasets (Zbinden et al., 2013; Staufer et al., 2013, 2014; Tanimoto et al., 2015; Tarasick et al., 2019). Staufer et al. (2013, 2014) used trajectory calculations to match air parcels sampled by both sondes and aircraft. Zbinden et al. (2013) compared coincidences (±24 hours) at three site pairs, while Tanimoto et al. (2015) examined simultaneous observations (±3 hours for sonde versus aircraft) at several site pairs less than 100 km apart. In general, these studies show small (6% or less) negative biases of aircraft measurements against ECC sondes. Tarasick et al. (2019) compared trajectory-mapped averages over 20°-70° N of ozonesonde and MOZAIC/IAGOS profiles and concluded that over 1994-2012 ozonesonde measurements were about $5 \pm 1\%$ higher in the lower troposphere and $8 \pm 1\%$ higher in the upper troposphere.

As shown above, the global O_3 vertical distribution datasets observed by WOUDC and IAGOS have been widely used in various studies. Still, a long-term and multi-site systematic comparison of these two datasets is rare, especially for the observations in the past three decades. In this study, we attempt to make the most comprehensive evaluation to date of the relative biases of IAGOS and sonde profiles, using as many station pairs as possible. We identify 23 suitable pairs of sites in the

88 WOUDC and IAGOS datasets from 1995 to 2021, compare the average vertical distribution of

89 tropospheric O_3 shown by ozonesonde and aircraft measurements, and analyze their differences by

90 ozonesonde type and by station-airport distance.

91

92 **2 Data and methods**

93 **2.1 MOZAIC-IAGOS observations**

94 The MOZAIC (Measurements of OZone and water vapor on Airbus In-service airCraft) program,

95 initiated in 1994 and incorporated into the IAGOS (In-service Aircraft for a Global Observing

96 System; www.iagos.org) program since 2011, takes advantage of commercial aircraft to provide

97 worldwide in-situ measurements of several trace gases (e.g., O_3 and CO) and meteorological

98 variables (e.g., water vapor) throughout the troposphere and the lower stratosphere (Marenco et al.,

99 1998; Petzold et al., 2015; Nédélec et al., 2015). O_3 measurements are performed using a dual-beam

100 UV-absorption monitor (time resolution of 4 seconds) with an instrumental uncertainty of ± 2

101 ppbv+2% (Thouret et al., 1998; Blot et al., 2021). It should be noted that this is only the instrumental

102 uncertainty, and does not include sampling uncertainties (possible losses) caused by the inlet line

103 and the compressor before the UV-photometric measurements are made. Loss of O_3 on the inlet

104 pump was an issue in earlier aircraft O_3 sampling programs (Brunner et al., 2001; Dias-Lalcaca et

105 al., 1998; Schnadt Poberaj et al., 2007; Thouret et al., 2022), but Thouret et al. (1998) found it

106 negligible for MOZAIC/IAGOS.

107 More details on the new IAGOS instrumentation can be found in Nédélec et al. (2015). The

108 continuity of the dataset between the MOZAIC and IAGOS programs has been demonstrated based

109 on their 2-year overlap (2011-2012) (Nédélec et al., 2015). Blot et al. (2021) evaluated the internal

110 consistency of the O_3 measurements since 1994, which confirmed the instrumental uncertainty of

111 ± 2 ppb. Moreover, they found no bias drift amongst the different instrument units (six O_3 IAGOS-

112 MOZAIC instruments, nine IAGOS-Core Package1 and the two instruments used in the IAGOS-

113 CARIBIC aircraft).

114 **2.2 WOUDC ozonesonde observations**

115 The World Ozone and Ultraviolet Radiation Data Centre (WOUDC) is part of the Global

116 Atmosphere Watch (GAW) program of the World Meteorological Organization

(https://woudc.org/data/explore.php). The WOUDC is operated by Environment and Climate Change Canada. WOUDC ozonesonde data have been evaluated in a number of WMO-sponsored international field intercomparisons (Attmannspacher and Dütsch, 1970, 1981; Kerr et al, 1994) and more recently in laboratory simulation chamber experiments using a standard reference photometer (Smit et al., 2007, 2024; Thompson et al., 2019). In the global ozonesonde network, while different ozonesonde types were common in the past, more than 95% of current sounding stations use electrochemical concentration cells (ECC). ECC ozonesondes have a precision of 3-5% (1-σ) while the precision of other sonde types is somewhat poorer, at about 5–10% for Brewer-Mast and the Japanese KC (Carbon-Iodine) sonde, and somewhat larger for the Indian-sonde (Kerr et al., 1994; Smit et al., 2007). Biases with respect to UV reference spectrometers have been estimated for ECC sondes at 1-5% in the troposphere (Smit et al., 2021; Tarasick et al., 2019, 2021).

2.3 Data processing

The two datasets were first screened for airport-sonde station pairs within a latitude separation of <4° and a longitude separation of <4°. Many sonde stations have observational records that do not overlap with the IAGOS period (1994-present). In addition, the IAGOS dataset has large gaps at many airports, because the frequency of visits to airports by aircraft that take part in IAGOS depends on commercial airlines' operating constraints. In total, 23 station pairs (Fig. 1) were identified with a separation of less than 4° in both latitude and longitude, and coincident observations over at least nine months. The majority of the 23 ozonesonde site records are ECC (17), while four are Indian-sonde, one Brewer-Mast, and one Carbon-Iodine (the Japanese KC sonde). These stations were divided into 3 groups according to the distance (D) between the ozonesonde station and the airport: D<1°, 1°<D<2°, and 2°<D<4°. Specific information on the comparison stations is shown in Table 1.

The observation times of the ozonesonde and aircraft are generally not the same. Ozonesondes are typically launched once a week, although a few stations have more frequent launches. The aircraft records generally contain more frequent observations, but observation times vary. For the selected 23 stations, we calculated the mean O_3 vertical profiles at 1km resolution (the first layer is from the surface to 1 km above sea level) for each month during the observational period for the two datasets. A minimum of four aircraft profiles were required to estimate a monthly mean profile; because

146 ozonesonde launches are typically only a few times per month, no minimum was required to

147 estimate a monthly mean profile. Only data with monthly means in both datasets were included for

148 further analysis. Comparisons between the two datasets were made by ozonesonde type and by

149 station-airport distance.

150

151 **3. Results and discussion**

152 **3.1 Comparison of the vertical profiles of tropospheric O_3 from four types of ozonesondes and**

153 **aircraft observations**

154 Previous intercomparisons of sondes launched on the same balloon (Attmannspacher and Dütsch,

155 1970, 1981; Beekmann et al, 1994, 1995; Deshler et al., 2008; Hilsenrath et al., 1986; Kerr et al,

156 1994; Smit et al., 2007) have shown that sondes of different types respond somewhat differently to

157 the same O_3 vertical profile; that is, they have relative biases, that vary with altitude. Fig. 2 therefore

158 compares the mean vertical profiles of tropospheric O_3 from ozonesonde and aircraft measurements,

159 separated by ozonesonde type. Both O_3 concentrations and absolute differences between

160 ozonesonde and aircraft increase with altitude, especially above 9 km. Average tropospheric O_3

161 profiles observed by ECC, Brewer-Mast, and Carbon-Iodine sondes are in good agreement with

162 aircraft measurements, with biases of 2.58 ppb, -0.28 ppb and 0.67 ppb, while the agreement with

163 the Indian-sonde is poorer, with a bias of 15.32 ppb. The Indian-sonde average also shows a linear

164 increase with altitude, while the aircraft measurements indicate an O_3 decrease with altitude above

165 8 km (Fig. 2b). This behavior is most clearly related to the comparisons of stations 2°-4° apart in

166 spring (Fig. S9).

167 These results are broadly consistent with those from JOSIE 1996 (Smit et al. 1996; Smit and Kley,

168 1998; Thompson et al., 2019), and with the northern hemisphere average result from Tarasick et al.

169 (2019). (Their Figure 20b; note that it is largely based on ECC sondes, and the scale is inverted

170 (IAGOS-sondes) from the sense we use here.)

171 Fig. 3 shows correlation plots of monthly mean O_3 at 1 km vertical intervals for months when both

172 IAGOS and ozonesonde data are available at the same location. While these monthly averages are

173 of data not necessarily coincident in time, Fig. 3 indicates that the data compare well on this

174 timescale, with correlation coefficients (R) of 0.71, 0.88 and 0.66, respectively (Fig. 3a-3c). The

175 agreement between the Indian-sonde and aircraft observations is poor, however, with an R of only

176 0.44 (Fig. 3d). The RMSE of O_3 observed with the four types of ozonesondes (ECC, Brewer-Mast,

177 Carbon-Iodine and Indian-sonde) and the aircraft is 15.99 ppb, 14.15 ppb, 16.26 ppb and 29.85 ppb,

178 respectively. After calculation, we obtained the slopes and offsets of ECC, Brewer-mast, Carbon-

179 iodine and Indian-sonde without forcing the fitted lines through zero, the slope is 0.71, 0.88, 0.56

180 and 0.74, respectively, and the offset is 18.94 ppb, 6.89ppb, 27.48ppb and 27.84ppb. When we force

181 the intercept to zero for the regressions, the slope is larger than the slope without forcing the fitted

182 lines through zero (fig. 3). In generally, when O_3 is zero both the ozonesondes and the aircraft will

183 measure zero. However, there is an offset in the fit of the two data sets due to potential causes for

184 systematic differences during the observation measurement process, e.g., high background current

185 in the sonde data.

186   Fig. 2 shows that the mean differences between ozonesonde and aircraft measurements vary

187 significantly with altitude. This can also be observed clearly from the relative differences (RD),

188 expressed as $(O_{3\text{-ozonesonde}} - O_{3\text{-aircraft}})/ O_{3\text{-aircraft}} \times 100\%$ (Fig. 4). O_3 concentrations from ECC

189 measurements are higher than those from aircraft measurements in all altitudes except at the surface.

190 Mean O_3 concentrations reported by Brewer-Mast sondes are lower than those from IAGOS below

191 7 km, but higher between 7 and 12 km. O_3 concentrations reported by Carbon-Iodine sondes are

192 higher than those observed from aircrafts below 2 km, but significantly lower above 8 km. In relative

193 terms, the bias between ECC sonde and aircraft measurements varies little with altitude, except near

194 the ground. The mean relative bias for Brewer-Mast measurements is at an absolute maximum of -

195 19 % near the ground, but increases slowly above 3 km, and is positive above 7 km, reaching more

196 than +10 % at 10-11 km. The relative bias for Carbon-Iodine measurements is about 8% below 2

197 km, becomes quite small from 2 - 8 km, and becomes large and negative above 8 km.

198 The Indian-sonde observations show much larger mean differences from the aircraft measurements.

199 Biases are everywhere positive, and as high as nearly 60% or 30 ppb, with much higher uncertainty

200 (standard errors) at each altitude as well (Fig. 2b, Fig. 4).

201 The region below 3 km has many local ozone sources and sinks (cities, airports, rural environment,

202 etc). In comparison, the region above 8 km is significantly influenced by stratosphere-troposphere

203 exchange, jet streams, and tropopause folds. Fig. S1 shows that the R between ozonesondes and

aircraft observations is higher near the ground (< 2 km) and at high altitudes (> 10 km). This shows that although the influencing factors of O_3 near the ground and at high altitudes are more complex, their long-term temporal variation characteristics are similar. The influences of cities, airports, rural environment, stratosphere-troposphere exchange, jet streams, tropopause folds, etc., have a more significant impact on the concentration of O_3 in the short term.

The correlation between four types of ozonesondes and aircraft observations also varies with altitude (Fig. S1). From 0-8 km, the correlation between ECC and aircraft observations decreases with altitude, with R being 0.71 at 0-1 km and reaching a minimum of 0.29 at 8-9 km; from 8-12 km, R increases with altitude, reaching 0.49 at 11-12 km. The correlation between the other three ozonesondes (Brewer-mast, Indian-sonde and Carbon-iodine) and the aircraft observations all vary with altitude, with different inflection points. The number of stations for these three types of ozonesondes is small (Table 1). Therefore, local variable influences on O_3 are more important, so R varies more with altitude.

The bias and RMSE with respect to the aircraft observations of the four types of ozonesondes at 8-12 km are higher than that at other altitudes. In contrast, the bias and RMSE values below 8 km are smaller and vary less with altitude, consistent with the vertical distribution characteristics of O_3 concentration in Fig. 2. This is likely due to the higher concentration of O_3 and the typically larger difference in spatial distance between ozonesonde and aircraft observations at 8-12km.

In addition, the bias and RMSE relative to the aircraft observations at different altitudes for ECC, Carbon-iodine and Brewer-mast sondes are lower than those for the Indian-sonde, which is similar to the results of the above analysis of O_3 concentration.

It should be noted that these comparisons only give an average relative bias between sondes and IAGOS. The true value of the ozone profile remains unknown, as do the absolute biases of sondes and IAGOS.

3.2 Seasonal variations in relative biases between ozonesondes and IAGOS

Fig. 5 compares mean profiles observed by ECC ozonesondes and IAGOS, separated by season. There are modest seasonal differences in the relative bias profiles, with somewhat larger average biases in winter and spring, but average biases are all positive (ECC sondes higher) and at all levels

233 the average seasonal biases are not statistically different.

234 The modest seasonal differences that are apparent in Fig. 5 and in Figs. S2-S4 are likely due to the

235 modest sample size (for ECC sondes) and small sample sizes (for other types). The actual

236 coincidence in time for profiles can range from less than one day to about 1-3 weeks, depending on

237 the number of ozonesonde and aircraft O_3 profiles collected within each month-bin. This means the

238 larger the atmospheric variability of O_3 is, the larger the real differences between ozonesonde and

239 aircraft O_3 can become, particularly when the number of profiles within a month-bin are small. In

240 addition, there are errors due to variations in the aircraft take-off and landing trajectories and the

241 balloon rise rate, the geographical location of the observation stations (and any associated

242 meteorological differences) and any systematic difference in standard observational times.

243 Table 2 indicates that in all four seasons ECC data correlate well with aircraft observations, with R

244 ranging from 0.71 to 0.76, but with larger average biases in winter and spring, as noted. It is not

245 clear if these seasonal average differences in bias are significant, as the uncertainty ranges on the

246 seasonal averages (lower plot of Fig. 5) overlap.

247 The vertical distribution of tropospheric O_3 observed by Brewer-Mast and IAGOS aircraft in the

248 four seasons is similar (Fig. S2). Differences are also similar, except above 7 km, where the

249 uncertainties are larger, and in general the uncertainty ranges on the seasonal difference averages

250 overlap. Since these comparisons come from only one station pair, some of the differences may be

251 attributable to local differences in topography and meteorology. Table 2 shows that correlations for

252 the ensemble of Brewer-Mast stations are higher than those for ECC stations. Like the ECC sondes,

253 average biases are all positive, but this is determined by the biases above 7 km (Fig. 4); unlike the

254 ECCs, biases are negative in the lowest 3 km.

255 The vertical distribution of tropospheric O_3 concentrations observed by Carbon-Iodine sondes and

256 IAGOS aircraft in the four seasons are similar, except in summer when the tropopause is high (Fig.

257 S3). The difference plots are fairly similar, except in the lowest 3 km, where differences become

258 quite large in summer. Like the previous comparison for Brewer-Mast sondes, these comparisons

259 come from only one station pair, and so the large differences in the boundary layer in summer are

260 likely due to local O_3 production sampled by the sonde but not the aircraft. Likely for this reason,

261 the consistency between Carbon-Iodine and aircraft observations is poor in summer, with R being

only 0.46 (Table 2). For the other three seasons it is fairly good.

The tropospheric O_3 observed by Indian-sondes displays a consistently high bias relative to IAGOS in all seasons, and the seasonal difference plots are quite similar, except in the lowest 3 km in winter (Fig. S4). This different behavior in winter is likely due to local ozone production sampled by the aircraft but not the sonde. Temperature inversions are common in the winter in northern India and trap local pollution. The very low values registered by the aircraft near the surface in summer also suggest local effects, in this case titration by NO_x.

The tropospheric O_3 observed by Indian-sonde in the four seasons is 43.3-79.4 ppb, 31.4-80.2 ppb, 42.2-69.6 ppb and 51.5-87.5 ppb, and that observed by aircraft in the four seasons is 22.8-60.1 ppb, 14.8-47.1 ppb, 25.0-44.1 ppb and 35.6-53.3 ppb (Fig. S4). The tropospheric O_3 observed in Indian-sonde in the four seasons increases with height almost linearly. The tropospheric O_3 observed by aircraft first increases and then decreases with altitude in spring, summer and autumn, while in winter, it first decreases and then increases with altitude. The tropospheric O_3 observed by the Indian-sonde and the aircraft is quite different, and the RD in the four seasons is 6.3% to 47.5%, 22.6% to 52.9%, 26.4% to 40.6% and 5.13% to 39.13%. Table 2 indicates poor consistency between Indian-sonde and aircraft observations in all four seasons, with R in winter only 0.18. The bias and RMSE in winter are the largest, at 40.07 ppb and 64.99 ppb. The bias, R and RMSE in the other three seasons are smaller, and the differences between them slight.

3.3 Dependence of relative biases on station-airport distances

A major concern with comparing IAGOS and ozonesonde observations is that the stations and airports are not generally co-located, and even where they are close, the flight paths taken by balloon and aircraft are quite different. Fig. 6 compares the average vertical distribution of tropospheric O_3 observed at different station-airport distances by ECC sondes and IAGOS aircraft. Note that we continue to separate sonde station data by type --- only ECC data are used here. Sonde-aircraft pairs have been grouped by station-airport distance (Table 1). The differences in average bias vary only very modestly between the different station-airport distance categories, and those differences are not statistically different at the 95% confidence level (Fig. 6d). This, partially owing presumably to the use of mean monthly averages, is encouraging, as this provides further evidence that the average bias we have derived is an artifact strictly of instrument differences.

291   Table 3 indicates that the bias variation between ECC and aircraft observations at different station-

292   airport distances is small, ranging from 5.7 ppb to 9.8 ppb. Correlations for these groupings are also

293   fairly similar, at R = 0.8, 0.9 and 0.7.

294   Compared with ECC sondes, the consistency between the Indian-sonde and aircraft observations is

295   poor at all station-airport distances, with much larger biases, and poor correlations, with R = 0.2 to

296   0.4. Nevertheless, Fig. S5 shows that the profiles of average differences are quite similar for station-

297   airport distances < 1°, and distances of 2°-4° (Fig. S5c).

298   Fig. 7 and Figs. S6-S8 examine possible seasonal variation in the differences at different station-

299   airport distances, for ECC sondes. The mean differences for the different station-airport distance

300   categories are larger than for the annual averages (Fig. 6), but in general those differences are not

301   statistically different at the 95% confidence level (Figs. 7d and S6d-S8d).

302

303   **3.4 Comparison of ozonesonde relative biases under operational conditions using IAGOS**

304   **observations as a transfer standard**

305   The foregoing discussion demonstrates that, consistent with previous work, there is a fairly constant

306   relative bias between IAGOS and sondes, with considerable dependence on sonde type, as expected

307   from previous sonde intercomparisons like JOSIE 1996. Although uncertainties are sizeable due to

308   the relatively sparse nature of the available data, we find consistent differences at all sites, with little

309   dependence on season or on station-airport separation, and little regional dependence (not shown).

310   Notwithstanding this overall sonde-IAGOS bias, we can use these station-airport comparisons to

311   derive relative biases of the different sonde types in use in the global network.

312   This does not assume that the aircraft data are unbiased. The true value of the O_3 profile (or even its

313   average) remains unknown, as do the absolute biases of sondes and IAGOS. It does assume:

314   1. That the measurement errors are random and normally distributed;

315   2. That there is one, constant bias for each measurement type (that is, if, for example, the Indian

316   sonde has changed over the period of comparison, or the IAGOS instruments have different biases,

317   there would be additional error that is not included in our uncertainty estimate);

318   3. That the measurement biases are not dependent on the geographic location or other variability of

319   the O_3 profile. This does not assume that the average O_3 profile is the same, just that the instruments

320   respond in the same way.

321   With these assumptions we can use the results of Fig. 2 to estimate the relative biases of each sonde

322   type to each other. The uncertainty of the comparisons will be the quadratic sum of the uncertainties

323   of the two IAGOS-sonde comparisons. The results are shown in Table 4. This intercomparison of

324   the different sonde types has an important advantage: it compares ozonesonde relative biases under

325   operational conditions, as it compares the data that are actually in databases like the WOUDC. It

326   also fills a gap, as the last WMO international intercomparison involving all four sonde types was

327   JOSIE 1996. These results are broadly consistent with those from JOSIE 1996 (Smit and Kley, 1998;

328   their Table 8 and Fig. 11).

329   In fact, the types of ozonesonde have changed during long-term observations at some stations (e.g.

330   Uccle and Payerne). De Backer et al. (1998) showed that with the use of an appropriate correction

331   procedure, accounting for the loss of pump efficiency with decreasing pressure and temperature, it

332   is possible to reduce the mean difference between O_3 profiles obtained with both types of sondes

333   below 3%, which is statistically insignificant over nearly the whole operational altitude range (from

334   the ground to 32 km). Stübi et al. (2008) also found that the O_3 difference between the Brewer-Mast

335   and the ECC ozonesonde data shows good agreement between the two sonde types, and the profile

336   of the O_3 difference is limited to $\pm5\%$ (±0.3 mPa) from the ground to 32 km. The results for Brewer-

337   Mast sondes in Table 4 should also be applicable to the older Payerne and Uccle records, and are

338   generally consistent with these results and with those for the older Canadian records (Tarasick et al.,

339   2002; 2016).

340   The results in Table 4 will be quite valuable for addressing the problem of relative biases when

341   merging ozonesonde data into global climatologies (e.g. McPeters et al., 2007; McPeters and Labow,

342   2012; Bodeker et al., 2013; Liu et al., 2013; Hassler et al., 2018;).

343   **4 Conclusions**

344   The vertical distribution of tropospheric O_3 observed by ozonesondes and IAGOS aircraft sensors

345   are compared at 23 pairs of sites between about 30°S and 55°N from 1995 to 2021. Overall, ECC,

346   Brewer-Mast, and Carbon-Iodine sondes agree reasonably well with aircraft observations, with

347   average biases of 2.58 ppb, -0.28 ppb, and 0.67 ppb, and correlation coefficients of 0.72, 0.82, and

348   0.66, respectively. The agreement between the aircraft and Indian-sonde observations is poor, with

349 an average bias of 15.32 ppb and R of 0.44. Ozonesondes and aircraft observations have smaller R

350 in the middle troposphere, but larger bias and RMSE in the upper troposphere. The bias and RMSE

351 relative to the aircraft observations at different altitudes for ECC, Carbon-iodine and Brewer-mast

352 sondes are lower than those for the Indian-sonde.

353 Notwithstanding this general agreement, all sonde types show significant average biases with

354 respect to IAGOS. The O_3 concentration observed by ECC sondes is on average higher by 5-10%

355 than that observed by IAGOS aircraft, and the relative bias increases modestly with altitude.

356 Seasonal variations in the relative bias are not in general statistically significant. The distance

357 between station and airport within 4° also has little effect on the comparison results. When the ECC

358 station pairs are grouped by station-airport distances of <1° (latitude and longitude), 1-2°, and 2-4°,

359 biases with respect to IAGOS measurements vary from 5.7 to 9.8 ppb, and correlations from 0.7 to

360 0.9.

361 Thus, the observed average relative bias between sondes and IAGOS found in this study, also noted

362 by previous authors (Zbinden et al., 2013; Staufer et al., 2013, 2014; Tanimoto et al., 2015; Tarasick

363 et al., 2019), is a robust result. Possible reasons for the difference include: side reactions that cause

364 sondes to produce excess iodine (Saltzman and Gilbert, 1959), and/or loss of O_3 on the inlet pump

365 that could cause IAGOS monitors to read low at pressures below 800 hPa. The latter was an issue

366 in earlier aircraft O_3 sampling programs (Schnadt Poberaj et al., 2007; Dias-Lalcaca et al., 1998;

367 Brunner et al., 2001), but Thouret et al. (1998) found it negligible for MOZAIC/IAGOS. A recent

368 intercomparison campaign at the World Calibration Centre for Ozone Sondes (WCCOS) in Julich

369 in June 2023 indicates that the pumps do not greatly influence the ozone IAGOS measurements

370 between 1000 and 200 hPa. The IAGOS-CORE O_3 measurements (Package 1 with pressurization

371 pumps) and IAGOS-CARIBIC O_3 measurements differ by less than 2%, and the WCCOS reference

372 UV photometer measurements are usually higher by 1-2% (to a maximum of 5%) compared to both

373 IAGOS instruments (Blot et al., 2021; Nédélec et al., 2015; Thouret et al., 2022). IAGOS-CARIBIC

374 does not have pressurization system, so that's why the good comparison between both IAGOS

375 systems means a lot.

376 However, as noted by Saltzman and Gilbert (1959), the differences in stoichiometry found at

377 different pH values imply that the chemistry of reaction of O_3 with KI is complex, involving

378 reactions that cause loss of iodine, as well as reactions other than the principal one that produce

379 additional iodine. Several authors have noted the existence of slow side reactions involving the

380 phosphate buffer, with a time constant of about 20 minutes, that may also increase the stoichiometry

381 from 1.0 (Tarasick et al., 2021, Smit et al., 2024). Furthermore, evaporation causes the concentration

382 of the sensing solution to increase, which can further enhance the stoichiometry, by concentrating

383 the phosphate buffer, and to a lesser degree, by increasing the concentration of the KI itself (Johnson

384 et al., 2002). These factors could contribute to the observed average relative bias between sondes

385 and IAGOS found in this study.

386 This result implies that care must be taken when merging ozonesonde and IAGOS measurement

387 datasets. While the aircraft and sonde measurements are often complementary, filling in important

388 spatial gaps that would otherwise exist if only one type were used, the records are not typically over

389 the same period, and so merging can introduce spurious jumps if relative biases are not taken into

390 account.

391 The importance of O_3 in the troposphere as an air pollutant and a greenhouse gas, and therefore of

392 accurate measurements of its temporal and spatial distribution implies that it will be important to

393 resolve the causes of this bias, and so further research involving more direct comparisons of IAGOS

394 instrumentation and ozonesondes, e.g. in the WCCOS chamber, are strongly recommended.

395 These results are also useful to evaluate the relative biases of the different sonde types in the

396 troposphere, using the aircraft as a transfer standard. This intercomparison of the different sonde

397 types has the advantage that it compares ozonesonde relative biases under operational conditions;

398 that is, the data that are actually in databases like the WOUDC. These results will be invaluable for

399 addressing relative biases when merging ozonesonde data into global climatologies (e.g. Bodeker

400 et al., 2013; Hassler et al., 2018; Liu et al., 2013; McPeters et al., 2007; McPeters and Labow, 2012).

401

402 **Competing interests.** The contact authors have declared that none of the authors has any competing

403 interests.

404 **Data availability.** The global ozone sounding data were acquired from the World Ozone and

405 Ultraviolet Radiation Data Center (http://www.woudc.org) operated by Environment Canada. The

406 IAGOS data are created with support from the European Commission, national agencies in Germany

407 (BMBF), France (MESR), and the UK (NERC), and the IAGOS member institutions

408 (http://www.iagos.org/partners).

409 **Author contributions. HW**: Data curation, Methodology, Validation, Visualization, Writing -

410 original draft preparation, Writing - review & editing, Funding acquisition. **LS**: Methodology,

411 Investigation, Writing - original draft. **DWT**: Data curation, Resources, Conceptualization,

412 Supervision, Writing - original draft preparation, Writing - review & editing. **JL**: Data curation,

413 Resources, Methodology, Conceptualization, Supervision, Writing - original draft preparation,

414 Writing - review & editing, Funding acquisition. **TZ**: Funding acquisition, Writing - review &

415 editing. **HGJS** and **RVM**: Writing - review & editing. **HGJS** and **RB**: Acquisition of IAGOS data,

416 Quality assessment IAGOS data.

417

418 **Acknowledgments.** We thank many whose dedication makes datasets used in this study possible.

419 The global O_3 sounding data were acquired from the World Ozone and Ultraviolet Radiation Data

420 Center (http://www.woudc.org) operated by Environment Canada, Toronto, Canada, under the

421 auspices of the World Meteorological Organization. Flight-based atmospheric chemical

422 measurements are from IAGOS. IAGOS is funded by the European Union projects IAGOS-DS and

423 IAGOS-ERI. The IAGOS data are created with support from the European Commission, national

424 agencies in Germany (BMBF), France (MESR), and the UK (NERC), and the IAGOS member

425 institutions (http://www.iagos.org/partners). The participating airlines (Lufthansa, Air France,

426 Austrian, China Airlines, Iberia, Cathay Pacific, Air Namibia, Sabena) supported IAGOS by

427 carrying the measurement equipment free of charge since 1994. We are also thankful to the Digital

428 Research Alliance of Canada at the University of Toronto for facilitating data analysis.

429

430 **Financial support.** This study was supported by the Natural Science and Engineering Council of

431 Canada (Grant No. RGPIN-2020-05163), the National Key Research and Development Program of

432 China (Grant No., 2022YFC3701204), the National Natural Science Foundation of China

433 (42275196 and 41830965), the Natural Science Foundation of Jiangsu Province (BK20231300), and

434 Wuxi University Research Start-up Fund for Introduced Talents (2023r035).

435

References

Attmannspacher, A., and Dütsch„ H.U., 1970. International ozone sonde intercomparison at the Observatory Hohenpeissenberg, Ber. Dtsch. Wetterdienstes, 120, 1-85.

Attmannspacher, A., and Dütsch, H.U., 1981. Second international ozone sonde intercomparison at the Observatory Hohenpeissenberg, Ber. Dtsch. Wetterdienstes, 157, 1-64.

Beekmann, M., Ancellet, G., Megie, G., Smit, H.G.J., Kley, D., 1994. Intercomparison campaign of vertical ozone profiles including electrochemical sondes of ECC and Brewer-Mast type and a ground based UV-differential absorption lidar. Journal of Atmospheric Chemistry, 19, 259-288. 19.

Beekmann, M., Ancellet, G., Martin, D., Abonnel, C., Duverneuil, G., Eideliman, F., Bessemoulin, P., Fritz, N., Gizard, E., 1995. Intercomparison of tropospheric ozone profiles obtained by electrochemical sondes, a ground based lidar and an airborne UV-photometer. Atmospheric Environment, 29(9), 1027-1042.

Bernhard, G.H., Bais, A.F., Aucamp, P.J., Klekociuk, A.R., Liley, J.B., McKenzie, R.L., 2023. Stratospheric ozone, UV radiation, and climate interactions. Photochemical and Photobiological Sciences, 1-53.

Blot, R., Nedelec, P., Boulanger, D., Wolff, P., Sauvage, B., Cousin, J.-M., Athier, G., Zahn, A., Obersteiner, F., Scharffe, D., Petetin, H., Bennouna, Y., Clark, H., Thouret, V., 2021. Internal consistency of the IAGOS ozone and carbon monoxide measurements for the last 25 years. Atmospheric Measurement Techniques, 14, 3935-3951, https://doi.org/10.5194/amt-14-3935-2021.

Bodeker, G. E., Hassler, B., Young, P. J., Portmann, R. W., 2013. A vertically resolved, global, gap-free ozone database for assessing or constraining global climate model simulations. Earth System Science Data, 5, 31-43, https://doi.org/10.5194/essd-5-31-2013.

Brunner, D., J. Staehelin, D. Jeker, H., Wernli, U. Schumann, 2001. Nitrogen oxides and ozone in the tropopause region of the Northern Hemisphere: Measurements from commercial aircraft in 1995/96 and 1997. Journal of Geophysical Research: Atmospheres, 106, 27673-27699.

Callis, L.B., Boughner, R.E., Natarajan, M., Lambeth, J.D., Baker, D.N., Blake, J.B., 1991. Ozone depletion in the high latitude lower stratosphere: 1979-1990. Journal of Geophysical Research:

465   Atmospheres, 96(D2), 2921-2937.

466 David, L.M. and Nair, P.R., 2013. Tropospheric column O_3 and NO_2 over the Indian region observed

467   by Ozone Monitoring Instrument (OMI): Seasonal changes and long-term trends. Atmospheric

468   Environment, 65, 25-39.

469 De Backer, H., De Muer, D., De Sadelaer, G., 1998. Comparison of ozone profiles obtained with

470   Brewer-Mast and Z-ECC sensors during simultaneous ascents. Journal of Geophysical

471   Research: Atmospheres, 103(D16), 19641-19648.

472 Deshler, T., Mercer, J.L., Smit, H.G., Stubi, R., Levrat, G., Johnson, B.J., Oltmans, S.J., Kivi, R.,

473   Thompson, A.M., Witte, J., Davies, J., 2008. Atmospheric comparison of electrochemical cell

474   ozonesondes from different manufacturers, and with different cathode solution strengths: The

475   Balloon Experiment on Standards for Ozonesondes. Journal of Geophysical Research:

476   Atmospheres, 113(D4), D04307, doi:10.1029/2007JD008975.

477 Dias-Lalcaca, P., Brunner, D., Imfeld, W., Moser, W., Staehelin, J., 1998. An automated system for

478   the measurement of nitrogen oxides and ozone concentrations from a passenger aircraft:

479   Instrumentation and first results of the NOXAR project. Environmental Science and

480   Technology, 32(20), 3228-3236.

481 Ebojie, F., Burrows, J.P., Gebhardt, C., Ladstätter-Weißenmayer, A., Von Savigny, C., Rozanov, A.,

482   Weber, M., Bovensmann, H., 2016. Global tropospheric ozone variations from 2003 to 2011

483   as seen by SCIAMACHY. Atmospheric Chemistry and Physics, 16(2), 417-436.

484 Fu, Y. and Tai, A.P.K., 2015. Impact of climate and land cover changes on tropospheric ozone air

485   quality and public health in East Asia between 1980 and 2010. Atmospheric Chemistry and

486   Physics, 15(17), 10093-10106.

487 García, O.E., Sanromá, E., Schneider, M., Hase, F., León-Luis, S.F., Blumenstock, T., Sepúlveda,

488   E., Redondas, A., Carreño, V., Torres, C., Prats, N., 2022. Improved ozone monitoring by

489   ground-based FTIR spectrometry. Atmospheric Measurement Techniques, 15(8), 2557-2577.

490 García, O.E., Schneider, M., Sepúlveda, E., Hase, F., Blumenstock, T., Cuevas, E., Ramos, R., Gross,

491   J., Barthlott, S., Röhling, A.N., Sanromá, E., 2021. Twenty years of ground-based NDACC

492   FTIR spectrometry at Izaña Observatory-overview and long-term comparison to other

493   techniques. Atmospheric Chemistry and Physics, 21(20), 15519-15554.

494   Gaudel, A., Cooper, O.R., Ancellet, G., Barret, B., Boynard, A., Burrows, J.P., Clerbaux, C., Coheur,

495   P.F., Cuesta, J., Cuevas, E., Doniki, S., 2018. Tropospheric Ozone Assessment Report: Present-

496   day distribution and trends of tropospheric ozone relevant to climate and global atmospheric

497   chemistry model evaluation. Elementa: Science of the Anthropocene, 6.

498   Gaudel, A., Cooper, O.R., Chang, K.L., Bourgeois, I., Ziemke, J.R., Strode, S.A., Oman, L.D.,

499   Sellitto, P., Nédélec, P., Blot, R., Thouret, V., 2020. Aircraft observations since the 1990s reveal

500   increases of tropospheric ozone at multiple locations across the Northern Hemisphere. Science

501   Advances, 6(34), eaba8272.

502   Gebhardt, C., Rozanov, A., Hommel, R., Weber, M., Bovensmann, H., Burrows, J.P., Degenstein,

503   D., Froidevaux, L., Thompson, A.M., 2014. Stratospheric ozone trends and variability as seen

504   by SCIAMACHY from 2002 to 2012. Atmospheric Chemistry and Physics, 14(2), 831-846.

505   Hassler, B., Kremser, S., Bodeker, G. E., Lewis, J., Nesbit, K., Davis, S. M., Chipperfield, M. P.,

506   Dhomse, S. S., Dameris, M., 2018, An updated version of a gap-free monthly mean zonal mean

507   ozone database. Earth System Science Data, 10, 1473-1490.

508   Hegarty, J., Mao, H., Talbot, R., 2009. Synoptic influences on springtime tropospheric O_3 and CO

509   over the North American export region observed by TES. Atmospheric Chemistry and

510   Physics, 9(11), 3755-3776.

511   Hilsenrath, E., Attmannspacher, W., Bass, A., Evans, W., Hagemeyer, R., Barnes, R., Komhyr, W.,

512   Mauersberger, K., Mentall, J., Proffitt, M., Robbins, D., 1986. Results from the balloon ozone

513   intercomparison campaign (BOIC). Journal of Geophysical Research: Atmospheres, 91(D12),

514   13137-13152.

515   Hoogen, R., Rozanov, V.V., Burrows, J.P., 1999. Ozone profiles from GOME satellite data:

516   Algorithm description and first validation. Journal of Geophysical Research:

517   Atmospheres, 104(D7), 8263-8280.

518   Hu, L., Jacob, D.J., Liu, X., Zhang, Y., Zhang, L., Kim, P.S., Sulprizio, M.P., Yantosca, R.M., 2017.

519   Global budget of tropospheric ozone: Evaluating recent model advances with satellite (OMI),

520   aircraft (IAGOS), and ozonesonde observations. Atmospheric Environment, 167, 323-334.

521   Hubert, D., Heue, K.P., Lambert, J.C., Verhoelst, T., Allaart, M., Compernolle, S., Cullis, P.D., Dehn,

522   A., Félix, C., Johnson, B.J., Keppens, A., 2021. TROPOMI tropospheric ozone column data:

geophysical assessment and comparison to ozonesondes, GOME-2B and OMI. Atmospheric Measurement Techniques, 14(12), 7405-7433.

Johnson, B.J., Oltmans, S.J., Vömel, H., Smit, H.G.J., Deshler, T., Kroeger, C., 2002. ECC Ozonesonde pump efficiency measurements and tests on the sensitivity to ozone of buffered and unbuffered ECC sensor cathode solutions. Journal of Geophysical Research: Atmospheres, 107(4393), 10-1029. doi: 10.1029/2001JD000557.

Keckhut, P., McDermid, S., Swart, D., McGee, T., Godin-Beekmann, S., Adriani, A., Barnes, J., Baray, J.L., Bencherif, H., Claude, H., di Sarra, A.G., 2004. Review of ozone and temperature lidar validations performed within the framework of the Network for the Detection of Stratospheric Change. Journal of Environmental Monitoring, 6(9), 721-733.

Kerr, J.B., Fast, H., McElroy, C.T., Oltmans, S.J., Lathrop, J.A., Kyro, E., Paukkunen, A., Claude, H., Köhler, U., Sreedharan, C.R., Takao, T., 1994. The 1991 WMO international ozonesonde intercomparison at Vanscoy, Canada. Atmosphere-Ocean, 32(4), 685-716.

Lefohn, A.S., Malley, C.S., Smith, L., Wells, B., Hazucha, M., Simon, H., Naik, V., Mills, G., Schultz, M.G., Paoletti, E., De Marco, A., 2018. Tropospheric ozone assessment report: Global ozone metrics for climate change, human health, and crop/ecosystem research. Elementa: Science of the Anthropocene, 6.

Li, K., Jacob, D.J., Liao, H., Qiu, Y., Shen, L., Zhai, S., Bates, K.H., Sulprizio, M.P., Song, S., Lu, X., Zhang, Q., 2021. Ozone pollution in the North China Plain spreading into the late-winter haze season. Proceedings of the National Academy of Sciences, 118(10), e2015797118.

Li, K., Jacob, D.J., Shen, L., Lu, X., De Smedt, I., Liao, H., 2020. Increases in surface ozone pollution in China from 2013 to 2019: anthropogenic and meteorological influences. Atmospheric Chemistry and Physics, 20(19), 11423-11433.

Liao, Z., Ling, Z., Gao, M., Sun, J., Zhao, W., Ma, P., Quan, J., Fan, S., 2021. Tropospheric ozone variability over Hong Kong based on recent 20 years (2000-2019) ozonesonde observation. Journal of Geophysical Research: Atmospheres, 126(3), e2020JD033054.

Liu, G., Liu, J., Tarasick, D.W., Fioletov, V.E., Jin, J.J., Moeini, O., Liu, X., Sioris, C.E., Osman, M., 2013. A global tropospheric ozone climatology from trajectory-mapped ozone soundings. Atmospheric Chemistry and Physics, 13(21), 10659-10675.

Logan, J.A., 1985. Tropospheric ozone: Seasonal behavior, trends, and anthropogenic influence. Journal of Geophysical Research: Atmospheres, 90(D6), 10463-10482.

Ma, Y., Ma, B., Jiao, H., Zhang, Y., Xin, J., Yu, Z., 2020. An analysis of the effects of weather and air pollution on tropospheric ozone using a generalized additive model in Western China: Lanzhou, Gansu. Atmospheric Environment, 224, 117342.

McPeters, R.D., Labow, G.J., Logan, J.A., 2007. Ozone climatological profiles for satellite retrieval algorithms. Journal of Geophysical Research: Atmospheres, 112(D5), D05308. doi:10.1029/2005JD006823.

McPeters, R.D. and Labow, G.J., 2012. Climatology 2011: An MLS and sonde derived ozone climatology for satellite retrieval algorithms. Journal of Geophysical Research: Atmospheres, 117(D10), D10303. doi:10.1029/2011JD017006.

Miles, G.M., Siddans, R., Kerridge, B.J., Latter, B.G., Richards, N.A.D., 2015. Tropospheric ozone and ozone profiles retrieved from GOME-2 and their validation. Atmospheric Measurement Techniques, 8(1), 385-398.

Meng, K., Zhao, T., Xu, X., Zhang, Z., Bai, Y., Hu, Y., Zhao, Y., Zhang, X., Xin, Y., 2022. Influence of stratosphere-to-troposphere transport on summertime surface O_3 changes in North China Plain in 2019. Atmospheric Research, 276, 106271.

Monks, P.S., Archibald, A.T., Colette, A., Cooper, O., Coyle, M., Derwent, R., Fowler, D., Granier, C., Law, K.S., Mills, G.E., Stevenson, D.S., 2015. Tropospheric ozone and its precursors from the urban to the global scale from air quality to short-lived climate forcer. Atmospheric Chemistry and Physics, 15(15), 8889-8973.

Nédélec, P., Blot, R., Boulanger, D., Athier, G., Cousin, J.M., Gautron, B., Petzold, A., Volz-Thomas, A., Thouret, V., 2015. Instrumentation on commercial aircraft for monitoring the atmospheric composition on a global scale: the IAGOS system, technical overview of ozone and carbon monoxide measurements. Tellus B: Chemical and Physical Meteorology, 67(1), 27791. https://doi.org/10.3402/tellusb.v67.27791@zelb20.2016.68.issue-s1

Percy, K.E., Legge, A.H., Krupa, S.V., 2003. Tropospheric ozone: a continuing threat to global forests? Developments in Environmental Science, 3, 85-118.

Perlwitz, J., Pawson, S., Fogt, R.L., Nielsen, J.E., Neff, W.D., 2008. Impact of stratospheric ozone

581   hole recovery on Antarctic climate. Geophysical Research Letters, 35(8).

582   https://doi.org/10.1029/2008GL033317.

583   Ramanathan, V., Cicerone, R.J., Singh, H.B., Kiehl, J.T., 1985. Trace gas trends and their potential

584   role in climate change. Journal of Geophysical Research: Atmospheres, 90(D3), 5547-5566.

585   Saltzman, B.E. and Gilbert, N., 1959. Iodometric microdetermination of organic oxidants and ozone.

586   Resolution of mixtures by kinetic colorimetry. Analytical Chemistry, 31(11), 1914-1920.

587   Schnadt Poberaj, C., Staehelin, J., Brunner, D., Thouret, V., Mohnen, V., 2007. A UT/LS ozone

588   climatology of the nineteen seventies deduced from the GASP aircraft measurement program.

589   Atmospheric Chemistry and Physics, 7(22), 5917-5936.

590   Schultz, M.G., Schröder, S., Lyapina, O., Cooper, O.R., Galbally, I., Petropavlovskikh, I., Von

591   Schneidemesser, E., Tanimoto, H., Elshorbany, Y., Naja, M., Seguel, R.J., 2017. Tropospheric

592   Ozone Assessment Report: Database and metrics data of global surface ozone

593   observations. Elementa: Science of the Anthropocene, 5.

594   Sharma, S., Sharma, P., Khare, M., 2017. Photo-chemical transport modelling of tropospheric ozone:

595   A review. Atmospheric Environment, 159, 34-54.

596   Smit, H.G.J., Sträter, W., Helten, M., Kley, D., Ciupa, D., Claude, H.J., Köhler, U., Hoegger, B.,

597   Levrat, G., Johnson, B., Oltmans, S.J., Kerr, J.B., Tarasick, D.W., Davies, J., Shitamichi, M.,

598   Srivastav, S.K., Vialle, C., 1996. JOSIE: The 1996 WMO international intercomparison of

599   ozonesondes under quasi-flight conditions in the environmental chamber at Jülich, *Proc.*

600   *Quadrennial Ozone Symposium 1996*, *l'Aquila, Italy,* edited by R. D. Bojkov and G. Visconti,

601   pp. 971-974, Parco Sci. e Tecnol. d'Abruzzo, Italy, 1996.

602   Smit, H.G., Straeter, W., Johnson, B.J., Oltmans, S.J., Davies, J., Tarasick, D.W., Hoegger, B., Stubi,

603   R., Schmidlin, F.J., Northam, T., Thompson, A.M., 2007. Assessment of the performance of

604   ECC-ozonesondes under quasi-flight conditions in the environmental simulation chamber:

605   Insights from the Juelich Ozone Sonde Intercomparison Experiment (JOSIE). Journal of

606   Geophysical Research: Atmospheres, 112(D19), D19306, doi:10.1029/2006JD007308.

607   Smit, H.G.J., 2014. Ozonesondes, in Encyclopedia of Atmospheric Sciences, Second Edition, edited

608   by G.R. North, J.A. Pyle, and F. Zhang, Vol 1, pp. 372–378, Academic Press, London.

609   Smit, H. G. J., Poyraz, D., Van Malderen, R., Thompson, A. M., Tarasick, D. W., Stauffer, R. M.,

Johnson, B. J., and Kollonige, D. E., 2024. New insights from the Jülich Ozone Sonde Intercomparison Experiment: calibration functions traceable to one ozone reference instrument. Atmospheric Measurement Techniques, 17, 73–112, https://doi.org/10.5194/amt-17-73-2024.

Smit, H.G.J., Thompson, A.M., and the ASOPOS 2.0 Panel, 2021. Ozonesonde Measurement Principles and 1300 Best Operational Practices, WMO Global Atmosphere Watch Report Series, No. 268, World Meteorological Organization, 1301 Geneva, [Available online at https://library.wmo.int/doc_num.php?explnum_id=10884].

Solomon, S., 1999. Stratospheric ozone depletion: A review of concepts and history. Reviews of Geophysics, 37(3), 275-316.

Staehelin, J., Harris, N.R., Appenzeller, C. and Eberhard, J., 2001. Ozone trends: A review. Reviews of Geophysics, 39(2), 231-290.

Staufer, J., Staehelin, J., Stübi, R., Peter, T., Tummon, F., Thouret, V., 2013. Trajectory matching of ozonesondes and MOZAIC measurements in the UTLS - Part 1: Method description and application at Payerne, Switzerland. Atmospheric Measurement Techniques, 6, 3393-3406. doi:10.5194/amt-6-3393-2013.

Staufer, J., Staehelin, J., Stübi, R., Peter, T., Tummon, F., Thouret, V., 2014. Trajectory matching of ozonesondes and MOZAIC measurements in the UTLS - Part 2: Application to the global ozonesonde network. Atmospheric Measurement Techniques, 7, 241-266. doi:10.5194/amt-7-241-2014.

Stübi, R., Levrat, G., Hoegger, B., Viatte, P., Staehelin, J., Schmidlin, F.J., 2008. In-flight comparison of Brewer-Mast and electrochemical concentration cell ozonesondes. Journal of Geophysical Research: Atmospheres, 113(D13). https://doi.org/10.1029/2007JD009091.

Tanimoto, H., Zbinden, R.M., Thouret, V., Nédélec, P., 2015. Consistency of tropospheric ozone observations made by different platforms and techniques in the global databases. Tellus B: Chemical and Physical Meteorology, 67(1), 27073.

Tarasick, D. W., Davies, J., Anlauf, K., Watt, M., Steinbrecht, W., Claude, H. J., 2002. Laboratory investigations of the response of Brewer-Mast ozonesondes to tropospheric ozone. Journal of Geophysical Research: Atmospheres, 107(D16), ACH-14, https://doi.org/10.1029/2001JD001167.

Tarasick, D. W., Davies, J., Smit, H. G., Oltmans, S. J., 2016. A re-evaluated Canadian ozonesonde record: measurements of the vertical distribution of ozone over Canada from 1966 to 2013. Atmospheric Measurement Techniques, 9(1), 195-214.

Tarasick, D.W., Galbally, I., Cooper, O.R., Schultz, M.G., Ancellet, G., LeBlanc, T., Wallington, T.J., Ziemke, J., Liu, X., Steinbacher, M., Stähelin, J., Vigouroux, C., Hannigan, J., García, O., Foret, G., Zanis, P., Weatherhead, E., Petropavlovskikh, I., Worden, H., Neu, J.L., Osman, M., Liu, J., Lin, M., Granados-Muñoz, M., Thompson, A.M., Oltmans, S.J., Cuesta, J., Dufour, G., Thouret, V., Hassler, B., Thompson, A.M., Trickl, T., 2019. TOAR- Observations: Tropospheric ozone from 1877 to 2016, observed levels, trends and uncertainties. Elementa: Science of the Anthropocene, 7(1), 39. DOI: http://doi.org/10.1525/elementa.376.

Tarasick, D.W., Smit, H.G., Thompson, A.M., Morris, G.A., Witte, J.C., Davies, J., Nakano, T., Van Malderen, R., Stauffer, R.M., Johnson, B.J., Stübi, R., Oltmans, S.J., Vömel, H., 2021. Improving ECC ozonesonde data quality: Assessment of current methods and outstanding issues. Earth and Space Science, 8, e2019EA000914. https://doi.org/10.1029/2019EA000914.

Thouret, V., Clark, H., Petzold, A., Nédélec, P., Zahn, A., 2022. IAGOS: Monitoring Atmospheric Composition for Air Quality and Climate by Passenger Aircraft. In Handbook of Air Quality and Climate Change (pp. 1-14). Singapore: Springer Nature Singapore.

Thouret, V., Marenco, A., Logan, J.A., Nédélec, P., Grouhel, C., 1998. Comparisons of ozone measurements from the MOZAIC airborne program and the ozone sounding network at eight locations. Journal of Geophysical Research: Atmospheres, 103(D19), 25695-25720. doi: 10.1029/98JD02243.

Thompson, A. M., Smit, H. G. J., Witte, J. C., Stauffer, R. M., Johnson, B. J., Morris, G., von der Gathen, P., Van Malderen, R., Davies, J., Piters, A., Allaart, M., Posny, F., Kivi, R., Cullis, P., Hoang Anh, N. T., Corrales, E., Machinini, T., da Silva, F. R., Paiman, G., Thiong'o, K., Zainal, Z., Brothers, G. B., Wolff, K. R., Nakano, T., Stübi, R., Romanens, G., Coetzee, G. J. R., Diaz, J. A., Mitro, S., Mohamad, M., Ogino, S., 2019. Ozonesonde quality assurance: The JOSIE-SHADOZ (2017) experience. Bulletin of the American Meteorological Society, 100(1), 155-171.

Vingarzan, R., 2004. A review of surface ozone background levels and trends. Atmospheric

668   Environment, 38(21), 3431-3442.

669   Vömel, H., Smit, H. G. J., Tarasick, D., Johnson, B., Oltmans, S. J., Selkirk, H., Thompson, A. M.,

670   Stauffer, R. M., Witte, J. C., Davies, J., van Malderen, R., Morris, G. A., Nakano, T., Stübi, R.,

671   2020. A new method to correct the electrochemical concentration cell (ECC) ozonesonde time

672   response and its implications for "background current" and pump efficiency, Atmospheric

673   Measurement Techniques, 13, 5667-5680, https://doi.org/10.5194/amt-13-5667-2020.

674   Wang, H., Ke, Y., Tan, Y., Zhu, B., Zhao, T., Yin, Y., 2023. Observational evidence for the dual roles

675   of BC in the megacity of eastern China: Enhanced O_3 and decreased $PM_{2.5}$

676   pollution. Chemosphere, 327, 138548.

677   Wang, H., Lu, X., Jacob, D.J., Cooper, O.R., Chang, K.L., Li, K., Gao, M., Liu, Y., Sheng, B., Wu, K.,

678   Wu, T., 2022. Global tropospheric ozone trends, attributions, and radiative impacts in 1995-2017:

679   an integrated analysis using aircraft (IAGOS) observations, ozonesonde, and multi-decadal

680   chemical model simulations. Atmospheric Chemistry and Physics, 22(20), 13753-13782.

681   Wang, T., Xue, L., Brimblecombe, P., Lam, Y.F., Li, L., Zhang, L., 2017. Ozone pollution in China:

682   A review of concentrations, meteorological influences, chemical precursors, and

683   effects. Science of the Total Environment, 575, 1582-1596.

684   Williamson, C.E., Neale, P.J., Hylander, S., Rose, K.C., Figueroa, F.L., Robinson, S.A., Häder, D.P.,

685   Wängberg, S.Å., Worrest, R.C., 2019. The interactive effects of stratospheric ozone depletion,

686   UV radiation, and climate change on aquatic ecosystems. Photochemical and Photobiological

687   Sciences, 18(3), 717-746.

688   Xu, J., Huang, X., Wang, N., Li, Y., Ding, A., 2021. Understanding ozone pollution in the Yangtze

689   River Delta of eastern China from the perspective of diurnal cycles. Science of the Total

690   Environment, 752, 141928.

691   Yang, T., Li, H., Wang, H., Sun, Y., Chen, X., Wang, F., Xu, L., Wang, Z., 2023. Vertical aerosol

692   data assimilation technology and application based on satellite and ground lidar: A review and

693   outlook. Journal of Environmental Sciences, 123, 292-305.

694   Young, P.J., Naik, V., Fiore, A.M., Gaudel, A., Guo, J., Lin, M.Y., Neu, J.L., Parrish, D.D., Rieder,

695   H.E., Schnell, J.L., Tilmes, S., 2018. Tropospheric Ozone Assessment Report: Assessment of

696   global-scale model performance for global and regional ozone distributions, variability, and

697   trends. Elementa: Science of the Anthropocene, 6.

698 Yu, R., Lin, Y., Zou, J., Dan, Y., Cheng, C., 2021. Review on atmospheric Ozone pollution in China:

699   Formation, spatiotemporal distribution, precursors and affecting factors. Atmosphere, 12(12),

700   1675.

701 Zang, Z., Liu, J., Tarasick, D., Moeini, O., Bian, J., Zhang, J., Thompson, A. M., Van Malderen, R., Smit,

702   H. G. J., Stauffer, R. M., Johnson, B. J., Kollonige, D. E., 2024. An improved Trajectory-mapped

703   Ozonesonde dataset for the Stratosphere and Troposphere (TOST): update, validation and

704   applications, EGUsphere [preprint], https://doi.org/10.5194/egusphere-2024-800, 2024.

705 Zbinden, R.M., Thouret, V., Ricaud, P., Carminati, F., Cammas, J.P., Nédélec, P., 2013. Climatology of

706   pure tropospheric profiles and column contents of ozone and carbon monoxide using MOZAIC in

707   the mid-northern latitudes (24° N to 50° N) from 1994 to 2009. Atmospheric Chemistry and Physics,

708   13(24), 12363-12388, https://doi.org/10.5194/acp-13-12363-2013, 2013.

709 Zhang, L., Jacob, D.J., Boersma, K.F., Jaffe, D.A., Olson, J.R., Bowman, K.W., Worden, J.R., Thompson,

710   A.M., Avery, M.A., Cohen, R.C., Dibb, J.E., 2008. Transpacific transport of ozone pollution and the

711   effect of recent Asian emission increases on air quality in North America: an integrated analysis

712   using satellite, aircraft, ozonesonde, and surface observations. Atmospheric Chemistry and

713   Physics, 8(20), 6117-6136.

714 Zhao, K., Huang, J., Wu, Y., Yuan, Z., Wang, Y., Li, Y., Ma, X., Liu, X., Ma, W., Wang, Y., Zhang,

715   X., 2021. Impact of stratospheric intrusions on ozone enhancement in the lower troposphere

716   and implication to air quality in Hong Kong and other South China regions. Journal of

717   Geophysical Research: Atmospheres, 126(18), e2020JD033955.

Figures
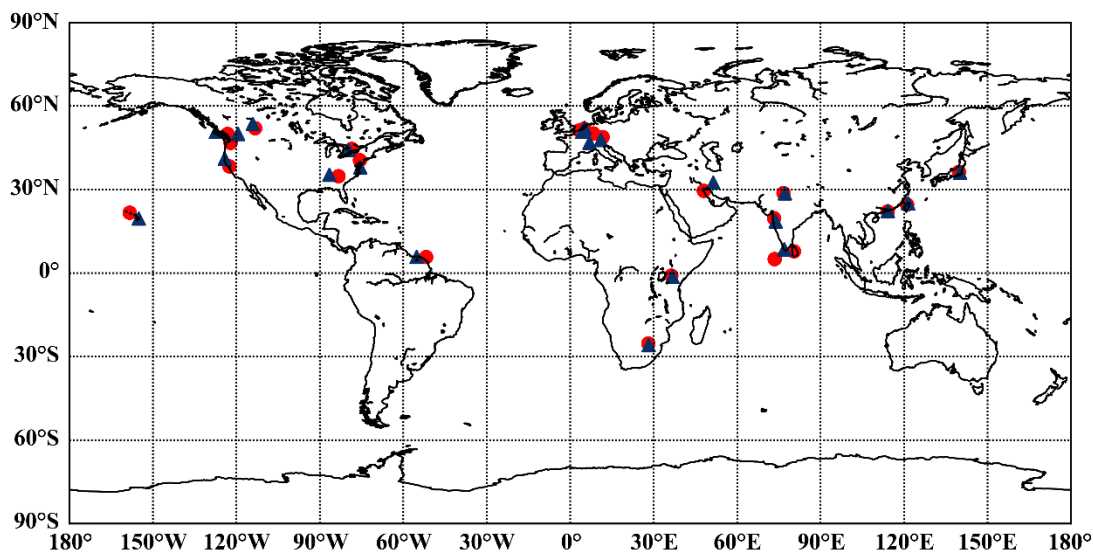
Figure 1. Map of 23 pairs of sites used in this study. Red circle markers are IAGOS sites, blue triangle markers are WOUDC sites.
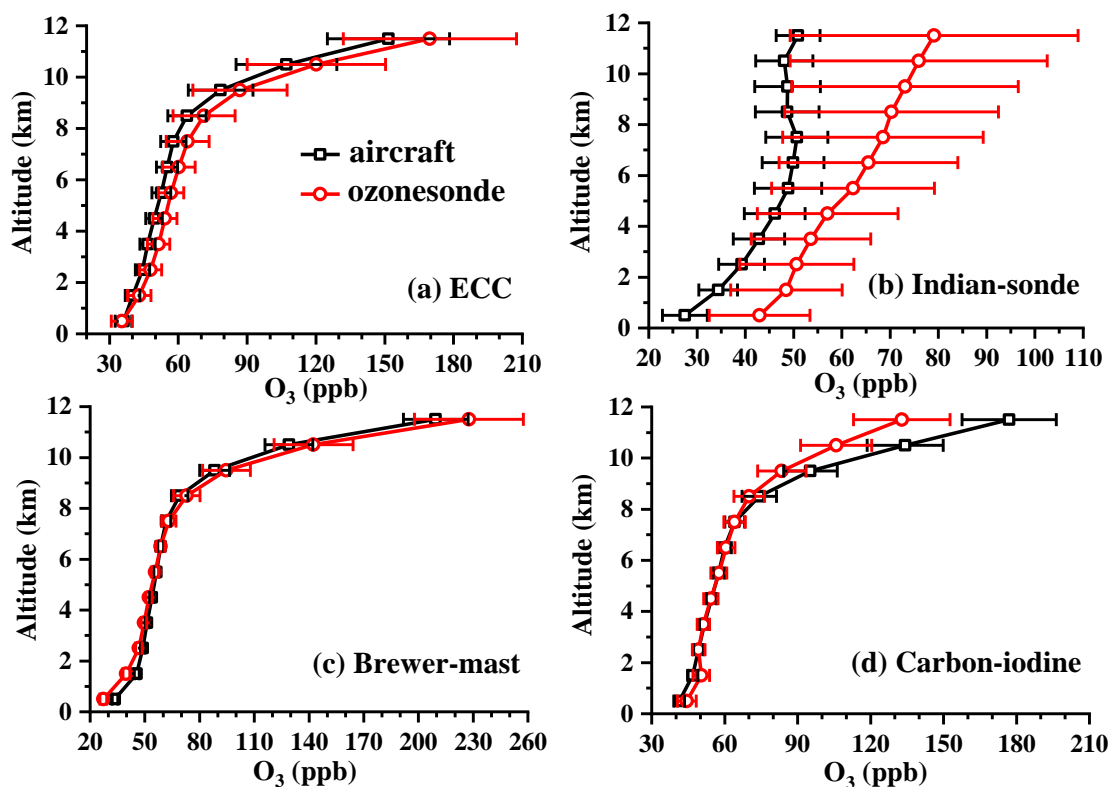
Figure 2. Comparison of the vertical profiles of tropospheric O_3 observed between aircraft measurements and four types of ozonesondes, ECC, Indian-sonde, Brewer-mast, and Carbon-iodine. The error bar length is 4 times the standard error (SE) of the mean (equivalent to 95% confidence limits on the averages).
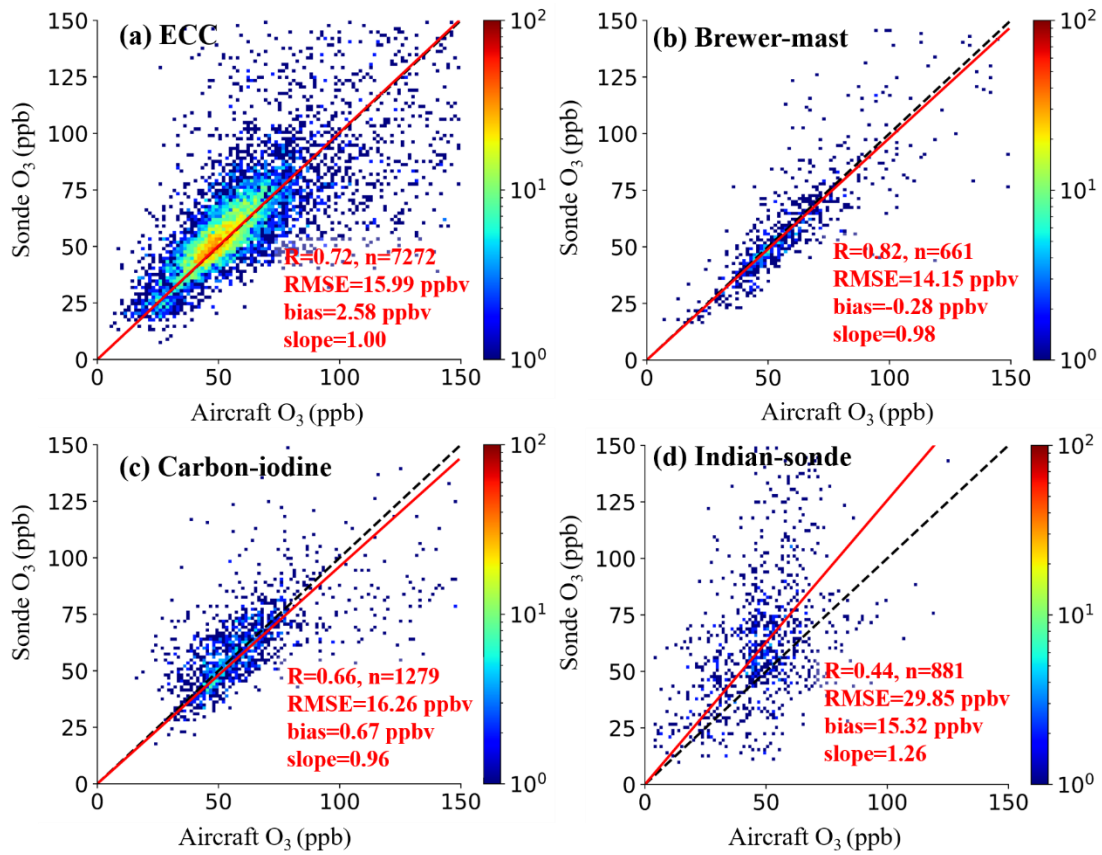
Figure 3. Correlation (*R*) of monthly mean ozone mixing ratios between ozonesonde and aircraft measurements. While IAGOS does measure in the lower stratosphere these values are usually far from the airport, so the sonde-aircraft distance will be large, we only plots data below 150 ppb. The black dashed line shows the 1:1 axis, the red line shows the linear fit (with the intercept set to 0), the color bar shows the data counts. Correlations are significant at the 99% level (*p* <0.01). *N* denotes the number of data points, R is the correlation coefficient, Bias is the overall average difference in monthly mean values [Ozonesonde ozone – Aircraft ozone, in ppb], RMSE is the root mean square error, slope is the slope of the linear fit line. All data points are based on the monthly mean.
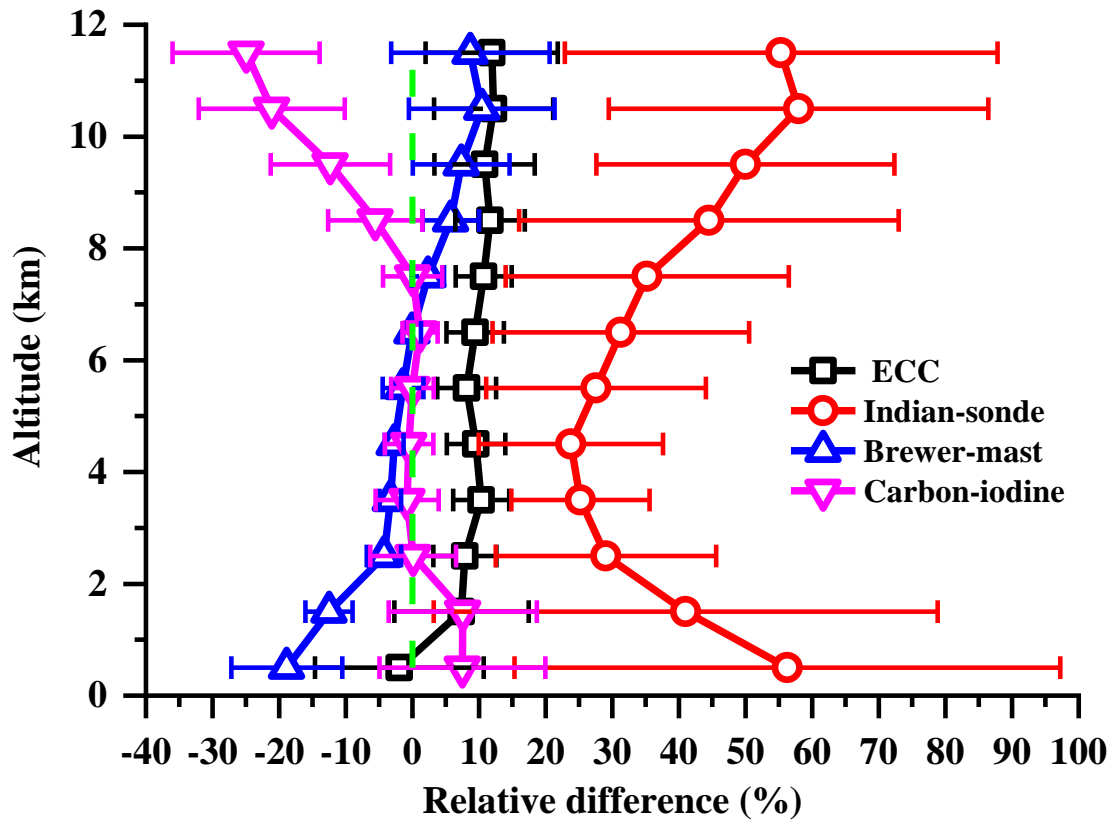
Figure 4. Mean relative difference (RD) between the ozonesonde O_3 and aircraft O_3 data. RD is calculated from ($O_{3\text{-ozonesonde}}$ - $O_{3\text{-aircraft}}$)/ $O_{3\text{-aircraft}}$×100%. The green dashed line is the zero line.
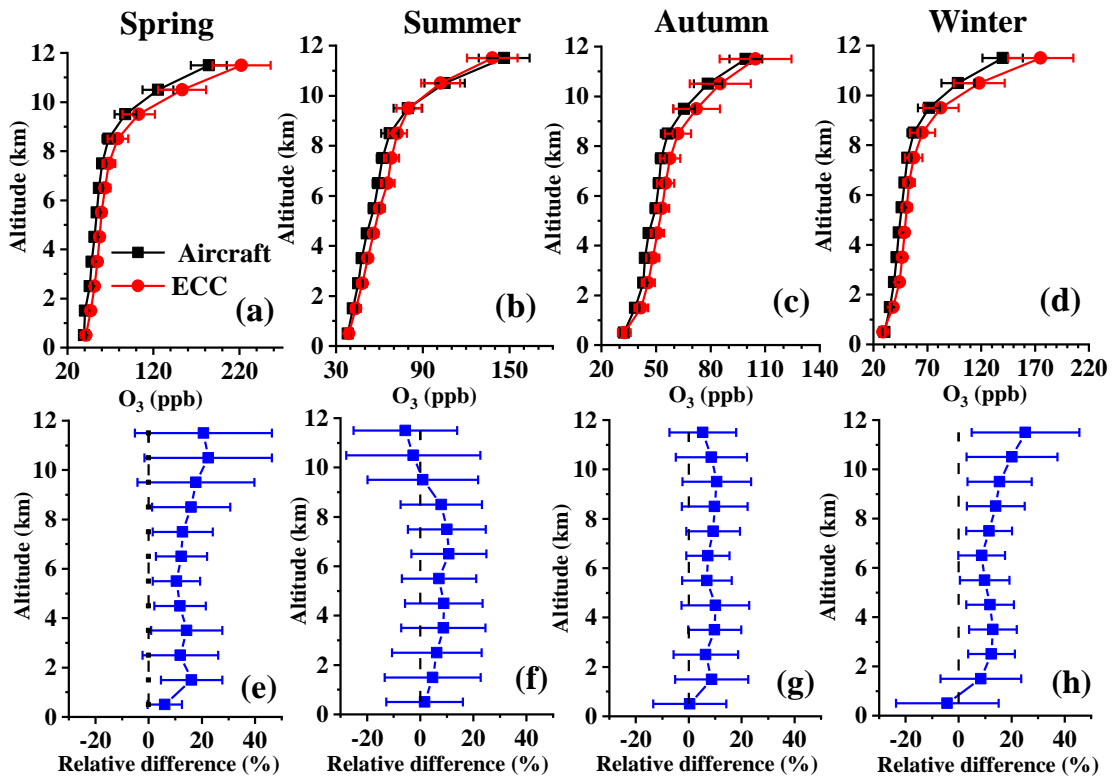
Figure 5. The mean difference in vertical profiles of the tropospheric O_3 between ECC ozonesonde and aircraft observations in four seasons (a-d) and their mean relative difference, the black dashed line is the zero line (e-h).
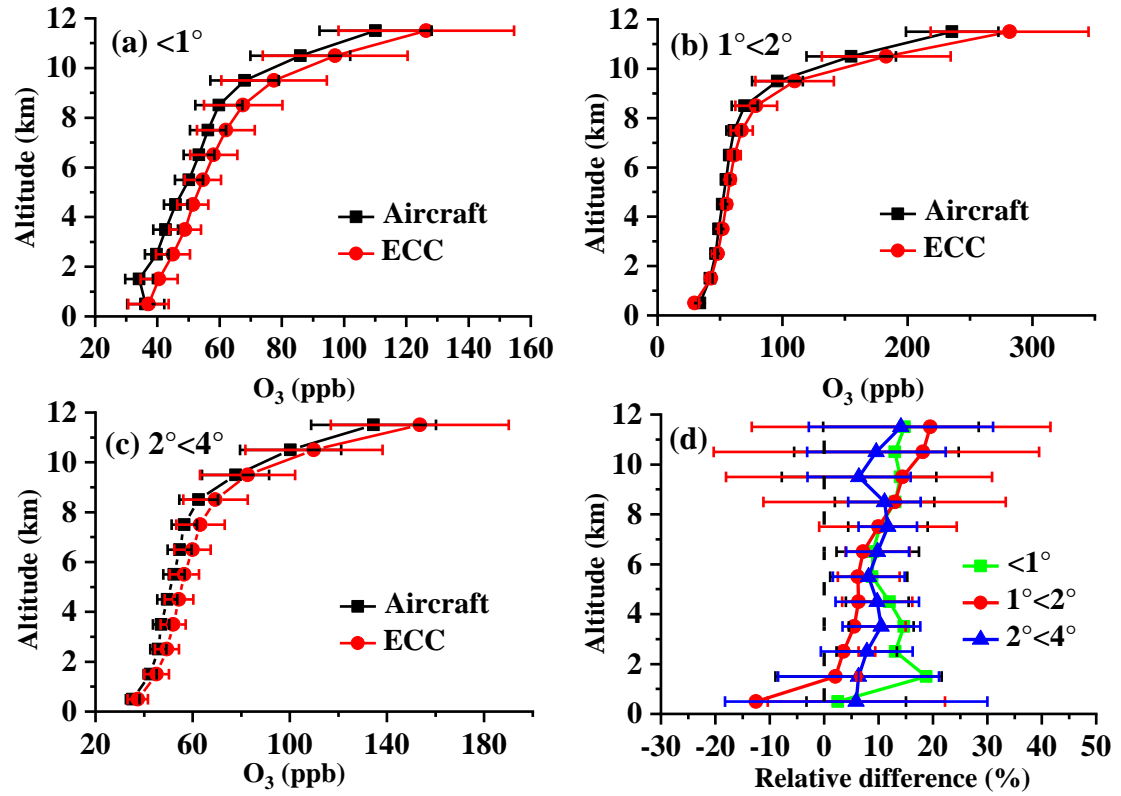
Figure 6. The annual mean vertical profiles of tropospheric O_3 between ECC ozonesonde and aircraft observations at station-pair distances (D) of D<1° (a), 1°< D <2° (b), and 2°< D <4°. The relative differences for the three categories are shown in (d), the black dashed line is the zero line.
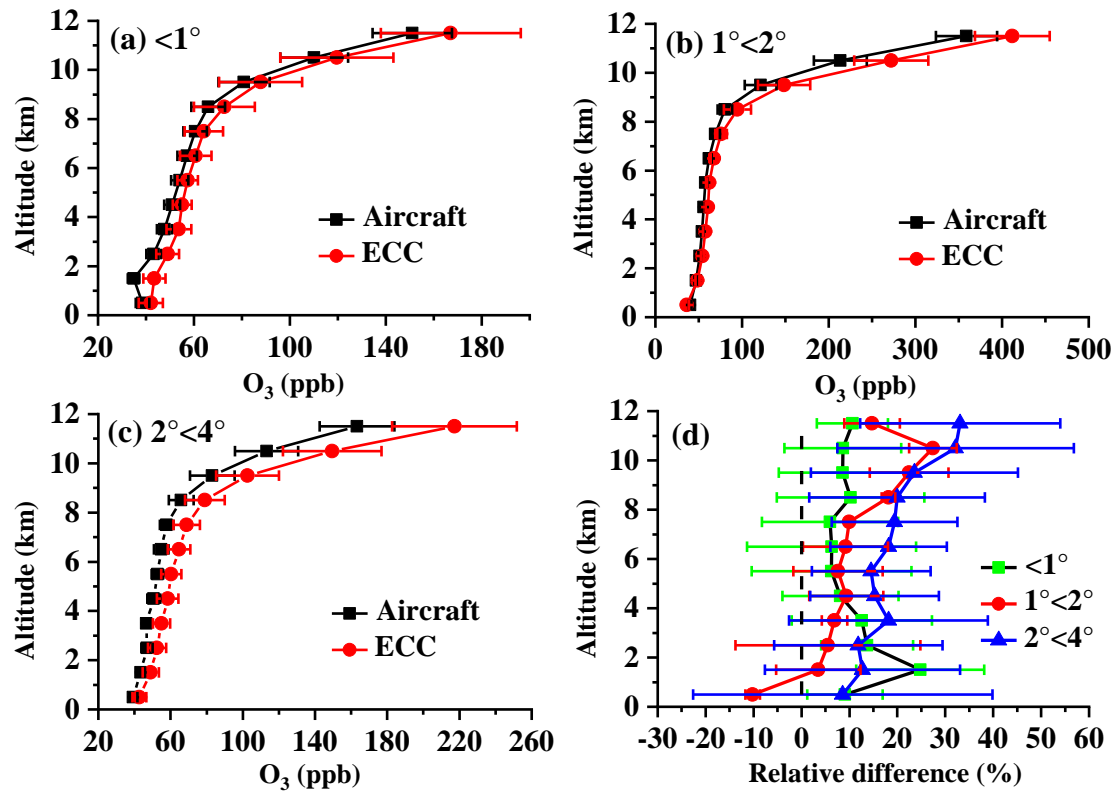
Figure 7. The seasonal mean vertical profiles of tropospheric O_3 in spring between ECC ozonesonde and aircraft observations at station-pair distances (D) of D<1° (a), 1°< D <2° (b), and 2°< D <4°.The relative differences for the three categories are shown in (d), the black dashed line is the zero line.

Tables

Table 1. Summary of the station information, including station's name, geolocation, the number of profiles, observational period, and the station-pair distance used in this study.

MOZAIC-IAGOS				WOUDC					Station-airport distance (km)	No. valid data months	observation period
Station name	Lon	Lat	No. profiles	Station name	Lon	Lat	No. profiles	Type			
Toronto	-78.50	44.58	321	Egbert	-79.78	44.23	181	ECC	108.87	33	2004-2008
Dusseldorf	4.96	51.82	412	De Bilt	5.18	52.10	333	ECC	34.59	63	1995-2013
Munich	11.78	48.35	2136	Hohenpeissenberg	11.02	47.81	1032	Brewer-mast	82.42	67	1996-2006
Johannesburg	28.07	-25.32	199	Irene	28.22	-25.91	135	ECC	67.30	26	1998-2003
Nairobi	36.33	-0.94	114	Nairobi	36.75	-1.30	42	ECC	61.50	10	1997-1998
Mumbai	73.26	19.05	122	Pune	73.85	18.53	56	Indian-sonde	84.85	35	1996-2003
Delhi	76.65	28.73	342	New Delhi	77.18	28.63	88	Indian-sonde	52.88	50	1995-2016
Hongkong	114.11	22.10	123	King's Park	114.17	22.31	115	ECC	24.15	25	2000-2005
Taipei	121.08	24.59	2115	Taipei	121.48	25.02	58	ECC	62.58	31	2014-2018
Tokyo	139.73	36.33	1342	Tateno (Tsukuba)	140.13	36.05	655	Carbon-iodine	47.52	116	1995-2006

Calgary	-113.25	52.03	170	Edmonton	-114.10	53.55	112	ECC	178.41	17	2009-2011
Brussels	3.24	51.21	2412	Uccle	4.36	50.80	736	ECC	148.40	55	1997-2009
Honolulu	-158.33	21.66	169	Hilo (HI)	-155.07	19.58	107	ECC	410.56	16	2015-2017
Vancouver	-123.14	49.95	595	Kelowna	-127.38	50.69	594	ECC	312.01	68	2003-2015
San-Francisco	-122.50	38.30	34	Trinidad Head (CA)	-124.15	41.05	53	ECC	336.78	10	1999-2001
Portland	-122.06	46.76	385	Kelowna	-119.38	49.97	317	ECC	408.08	45	2003-2009
Atlanta	-83.28	34.78	34	Huntsville (AL)	-86.58	35.28	85	ECC	305.54	10	1999-2006
Washington	-75.59	40.52	610	Wallops Island (VA)	-75.46	37.94	616	ECC	287.09	80	1994-2014
Cayenne	-51.78	5.75	200	Paramaribo	-55.21	5.81	64	ECC	379.50	9	2002-2013
Frankfurt	8.30	50.16	12742	Payerne	6.94	46.81	2673	ECC	385.72	204	2002-2020
Kuwait-City	48.01	29.52	105	Esfahan	51.43	32.48	34	ECC	463.15	17	2001-2004
Male	73.51	5.00	76	Trivandrum	76.95	8.48	45	Indian-sonde	543.73	24	1997-2000
Colombo	80.41	7.79	31	Trivandrum	76.95	8.48	37	Indian-sonde	388.49	11	1998-2000

1 **Table 2.** Bias, correlation coefficient (R), and RMSE for four types of ozonesonde and aircraft

2 observations in four seasons.

Type	Season	Bias ($O_{3\text{-ozonesonde}}$ - $O_{3\text{-aircraft}}$) (ppb)	R	RMSE (ppb)
ECC	Spring	17.34	0.76	65.52
	Summer	1.96	0.76	40.15
	Autumn	1.75	0.71	34.47
	Winter	7.61	0.71	51.74
Brewer-mast	Spring	10.22	0.94	43.51
	Summer	2.99	0.83	48.79
	Autumn	6.53	0.79	29.40
	Winter	6.11	0.88	45.45
Carbon-iodine	Spring	-9.19	0.84	38.34
	Summer	3.83	0.46	29.31
	Autumn	2.33	0.68	15.10
	Winter	-16.68	0.88	44.72
Indian-sonde	Spring	19.64	0.44	44.30
	Summer	19.58	0.57	37.44
	Autumn	20.38	0.45	37.30
	Winter	40.07	0.18	64.99

4 **Table 3**. Bias, correlation coefficient(R) and RMSE for ECC and Indian-sonde ozonesonde and

5 aircraft observations at different station-airport distances.

Type	Station-pair distance	Bias ($O_{3\text{-ozonesonde}}$ - $O_{3\text{-aircraft}}$) (ppb)	R	RMSE (ppb)
ECC	<1°	9.78	0.78	47.46
	1°-2°	8.91	0.90	40.73
	2°-4°	5.65	0.67	51.00
Indian-sonde	<1°	26.71	0.37	49.54
	2°-4°	15.35	0.24	30.86

7   **Table 4**. Comparison of the sondes of each type to IAGOS. (average ± 2 times the standard error

8   (SE)) Indian-sonde/ECC is (Indian-sonde/IAGOS)/(ECC/IAGOS), Brewer-mast/ECC is (Brewer-

9   mast/IAGOS)/(ECC/IAGOS), Carbon-iodine/ECC is (Carbon-iodine /IAGOS)/(ECC/IAGOS)

Altitude(km)	Indian-sonde/ECC	Brewer-mast/ECC	Carbon-iodine/ECC	ECC/ IAGOS
0-1	1.59 ±1.74	0.83 ±0.96	1.10 ±1.36	0.98 ±1.28
1-2	1.31 ±1.83	0.81 ±0.90	1.00 ±1.05	1.07 ±1.58
2-3	1.20 ±1.62	0.89 ±0.97	0.93 ±0.85	1.08 ±1.54
3-4	1.14 ±1.57	0.88 ±0.94	0.90 ±0.87	1.10 ±1.48
4-5	1.13 ±1.61	0.89 ±1.02	0.91 ±0.99	1.10 ±1.44
5-6	1.18 ±1.76	0.91 ±1.05	0.92 ±1.04	1.08 ±1.37
6-7	1.20 ±1.89	0.91 ±1.00	0.92 ±0.82	1.09 ±1.54
7-8	1.22 ±1.92	0.92 ±0.94	0.90 ±0.64	1.11 ±1.69
8-9	1.29 ±2.09	0.95 ±0.99	0.85 ±0.55	1.12 ±1.61
9-10	1.35 ±2.35	0.97 ±1.09	0.79 ±0.62	1.11 ±1.46
10-11	1.41 ±3.26	0.98 ±1.21	0.70 ±0.68	1.12 ±1.37
11-12	1.39 ±4.61	0.97 ±1.19	0.67 ±0.72	1.12 ±1.42